Acta Neuropathol (Berl) (1986) 70:60–70

Acta Neuropathologica

A Morphometric Study of Human Fetal Sural Nerve*

L. K. Shield**, R. H. M. King, and P. K. Thomas

Department of Neurological Science, Royal Free Hospital School of Medicine, Rowland Hill Street, London NW3 2PF, UK

Summary. A morphometric study was performed on sural nerves from human fetuses at 15 to 36 weeks postovulation. There were no myelinated fibres at 15 and 16 weeks, but by 21 weeks there were 5,000/mm^2, rising to 25,000/mm^2 at 36 weeks. During the fetal period, the mean myelin lamellar count trebled and the g ratio (axon diameter: total fibre diameter) decreased from 0.90 to 0.75, although the axon diameter of myelinated fibres did not increase. The smallest myelinated axon diameter was 0.63 μm, whereas the largest unmyelinated axon in a 1:1 relationship with a Schwann cell was 2.83 μm, suggesting that axon size is unlikely to be the only stimulus for myelination. The density of unmyelinated axons that were the sole occupants of a Schwann cell fell considerably between 23 and 33 weeks, while the ratio of total unmyelinated axons to myelinated fibres decreased from 82:1 at 21 weeks to 6:1 at 36 weeks. Data for Schwann cell nuclear density and percentages of fibres cut through the nucleus are also presented.

Key words: Fetal nerve – Sural nerve – Nerve development – Myelination – Nerve morphometry

Introduction

There have been relatively few reports of human fetal peripheral nerve development. Early studies such as those of Cravioto (1965), Gamble and Breathnach (1965), Dunn (1970), Davison et al. (1973) and subsequently those of Wozniak and O'Rahilly (1981) and Wozniak et al. (1982) were primarily descriptions of changing relationships between axons and Schwann cells and only limited (albeit valuable) quantitative analyses were performed.

In adult life, the use of sural nerve biopsy in the assessment of peripheral neuropathies led to a need for more morphometric data on mature and ageing peripheral nerve and this information, although still not complete, became available (Dyck 1966; Ochoa and Mair 1969a, b; Behse et al. 1972; Jacobs and Love 1985). These reports did not give an insight into the changes taking place during peripheral nerve development and the data obtained could not be validly used for comparison with pathological material from infants or children. Recognizing these deficiencies, Gutrecht and Dyck (1970) provided useful quantitative data on the sural nerve in the first two decades of life, the youngest nerve being from a 5 week premature infant. At the same time, Ochoa (1971) published more quantitative information from light and electron microscope studies on the sural nerve in 9- to 18-week-old fetuses. The studies by Tohgi et al. (1977), Schröder et al. (1978) and Origuchi (1981) have subsequently dealt with varying aspects of sural nerve development from the last 4 months of pregnancy onwards, but large gaps in knowledge still remain.

Undoubtedly the difficulty in obtaining suitably fixed material from human fetuses has contributed to the relative paucity of quantitative information on human nerve development. On the other hand, modern image analysis systems have facilitated the collection and interpretation of data.

This study of human fetal nerve was undertaken to define further some morphometric aspects of intrauterine nerve development and to provide baseline data for use in the evaluation of pathological processes affecting the fetus and young infants.

Offprint requests to: Prof. P. K. Thomas (address as above)

* Supported by the Friedreich's Ataxia Group, and by grants from Ciba-Geigy Ltd., Basel and the London University Central Equipment Fund for the purchase of image analysis equipment

** *Present address:* Department of Neurology, Royal Children's Hospital, Melbourne, Victoria, Australia

Table 1. Details of specimens

Nerve	Age postovulation (weeks)	Main method for assessment of age	Sex	Comments	Postmortem delay (h)
1	15	Foot length	M	Termination of pregnancy – normal fetus	0.25
2	16	Foot length	M	Termination of pregnancy – normal fetus	1
3	21	Crown-rump length	?	Termination of pregnancy – normal fetus	0.25
4	22	Foot length	M	Spontaneous miscarriage – normal fetus	7
5	23	Ultrasound	F	Spontaneous miscarriage – normal fetus	2
6	33	Foot length	M	Diaphragmatic hernia incomplete intestinal rotation	90
7	34	Foot length	F	Road trauma – normal fetus	48
8	36	Maternal dates	F	Spontaneous onset of labour Died aged 12 h – multiple congenital anomalies (anophthalmia, holoprosencephaly); limbs normal	2

Materials and Methods

Material

The sural nerve at mid-calf level was dissected at autopsy from 8 fetuses of 15–36 weeks postovulation age (Table 1). These age assignments were primarily based on measurements of fetal foot length (Streeter 1920) when available; otherwise fetal ultrasound data, crown-rump length or menstrual history were used. The time between death or spontaneous miscarriage and removal of the nerves varied from 15 min to 90 h. Parts of some nerves showed postmortem autolytic changes and hence not all measurements were performed on all nerves. Data are presented only for those parameters which could be measured in areas reasonably free of autolytic changes or when the presence of fibre distortion was not relevant (e.g., in counting numbers of fibres or nuclei). The problems in obtaining adequately fixed fetal material, particularly during the latter part of gestation, do not require further emphasis.

Tissue Processing

Specimens were fixed in 3% distilled glutaraldehyde in PIPES buffer with 2% sucrose for 1 to 3 days, following which they were washed in PIPES buffer for a minimum of 1 h and postfixed in 1% osmium tetroxide in the same buffer with 2% sucrose and 1.5% potassum ferricyanide for 3 h. After dehydration in increasing concentrations of ethanol, the specimens were embedded in Araldite (EMScope CY212) via 1–2 epoxypropane.

Semithin (1 μm) sections of the Araldite blocks were stained with thionin and acridine orange (Sievers 1971) for light microscopy and ultrathin sections for electron microscopy (Jeol 100CX) with 12% methanolic uranyl acetate and lead citrate.

Morphometry

A Kontron Videoplan quantitative digital image analyser was used for all measurements. The cursor was used to trace axon circumferences (taken as the internal circumference of the myelin sheath if there was axonal shrinkage) and from this the software program calculated the diameter of a circle with the same area. Hence the axon diameters reported here are derived values. For g ratio calculations (g = axon diameter : total fibre diameter; Schmitt and Bear 1937), myelin sheath thickness was derived by multiplying the lamellar count (number of major dense lines) by the intraperiod distance measured directly from 20 well-preserved fibres from each nerve. The electron microscope was calibrated using a diffraction grating replica of 2,160 lines/mm.

Transverse semithin sections were used to calculate myelinated fibre density and myelinated axon diameters. The Kontron cursor was used to measure the images displayed on a TV screen from a Leitz Orthoplan fitted with a TV camera and an oil immersion lens (×100). Electron micrograph photographic montages (at final magnifications of ×9,000, ×14,000 or ×19,800) were used for measurements of myelinated fibre density, unmyelinated fibre density, unmyelinated axon diameters, counts of the number of axons per Schwann cell or Schwann cell subunits (Sharma and Thomas 1975) and Schwann cell nuclear counts. Axon perimeter measurements (and hence the derived diameters) for g ratio calculations were taken from photographic negatives (magnification ×8,300, ×10,000 or ×13,000) of individual fibres representative of the axon diameter spectrum, while myelin lamellar counts and measurements of intraperiod distance were obtained by further magnifying these negatives and displaying a positive image on a TV screen.

The Kontron statistics program provided a *U*-Test for comparison of median values of two groups of measurements without the prerequisite of a Gaussian distribution.

Terminology

The terminology employed for unmyelinated fibres by Sharma and Thomas (1975) and Behse et al. (1975) has been adopted here. An *unmyelinated fibre* consists of a Schwann cell with its associated axons. An isolated Schwann cell process or group of processes, seen in transverse section and surrounded by basal lamina, whether or not associated with unmyelinated axons, is referred to as a *Schwann cell subunit*. In the present paper, *solitary* unmyelinated axons were those occurring in isolation, related to a Schwann cell perikaryon or subunit. *Aggregates* of unmyelinated axons consist of two or more adjacent axons "packaged" by Schwann cell processes. Because of the organization of human unmyelinated fibres with many solitary axons related to cell processes radiating from the Schwann cell perikaryon (Eames and Gamble 1970), it was not possible to identify "promyelin fibres" reliably (Friede and Samorajski 1968), i.e., unmyelinated axons segregated during development with a 1 : 1 relationship to a Schwann cell and destined to become myelinated.

Table 2. Myelinated fibre morphometry

Age (weeks)	Fibre density (per mm^2)		Axon diameters (μm) L/M			Lamellar counts			Mean g ratio (30–100)[a]
	L/M (218–1,464)[a]	E/M (25–273)[a]	Mean (218–1,464)[a]	Minimum	Maximum	Mean	Minimum (30–100)[a]	Maximum	
21	5,222	6,841	1.80	0.92	4.05	9.3	3	17	0.90
22	7,841	9,488	1.45	0.63	2.96	10.3	4	18	0.85
23	13,274	16,271	1.77	0.74	4.22	13.4	3	26	0.86
33	17,818	27,860	–	–	–	22.0	13	41	0.74
34	17,606	–	1.98	0.84	3.86	20.3	6	34	0.78
36	24,980	23,351	1.86	0.63	3.73	26.8	6	53	0.75

[a] Number of fibres counted
L/M = light microscopy; E/M = electron microscopy

Results

(a) Myelinated Fibres

Light microscopy. No myelinated fibres were present in the nerves at 15 and 16 weeks. Well-myelinated fibres were plentiful (5,000 mm^2) by 21 weeks, increasing up to 25,000/mm^2 at 36 weeks. Table 2 shows myelinated fibre densities, together with minimum, maximum and mean axon diameters. Myelinated axon diameter frequency distribution bar charts (Fig. 1) were unimodal for all nerves.

Electron microscopy. Myelinated fibre densities calculated from electron micrographs are shown in Table 2. They were in general slightly greater than those obtained by light microscopy; a major difference was only observed from the 33-week fetus. The differences presumably reflect the greater ease in the identification of smaller fibres by electron microscopy, variations in intrafascicular density and bias in selecting areas for electron microscope study, as areas including blood vessels or perineurial subdivisions were avoided.

Lamellar counts and g ratios. Minimum, maximum and mean lamellar counts and mean g ratios are given in Table 2. The maximum and mean lamellar counts increased threefold over the 21- to 36-week period. The mean g ratio showed a progressive decline from 0.9, indicating a thin myelin sheath relative to axon diameter, to 0.75, showing that myelin thickness increased in relationship to axon diameter. There was no statistically significant difference between median lamellar counts at 21, 22 and 23 or at 33, 34 and 36 weeks, but the difference between 23 and 33 weeks ($P < 0.001$) was significant. For g ratios, the only difference between medians that did not reach statistical significance was for 22 and 23 weeks. Values of $P < 0.001$ were found for differences between 21 and 22 weeks, and 23 and 33 weeks, whereas P was < 0.05 for 33 and 34 weeks and for 34 and 36 weeks.

Attempts to correlate lamellar counts and g ratios to axon diameters for individual nerves produced conflicting results. Fig. 3 shows that for nerves at 21, 23 and 36 weeks there appears to be correlation between increasing axon diameter and lamellar count but none at 22, 33 and 34 weeks. Similarly, for g ratios there was a correlation with increasing axon diameter for nerves at 22, 33 and 34 weeks but not at the other ages studied (Fig. 4). The post-mortem delay at 33 and 34 weeks was considerable but the 22-week nerve was fixed after only 7 h.

(b) Unmyelinated Fibres

All values were obtained from electron micrographs.

"Solitary" unmyelinated axons. Details for axon densities and for minimum, maximum and mean axon diameters, are shown in Table 3. A substantial difference in the density of solitary or isolated unmyelinated axons is seen between 15 and 16 weeks, but it should be noted that these densities are based on counts of only 5 and 212 axons respectively. There was a major decrease in density between 23 and 33 weeks. At the same time the ratio of solitary unmyelinated to myelinated fibres fell (Table 4), whereas the density of aggregates of unmyelinated axons (i.e., two or more axons segregated by Schwann cell processes) did not (Table 3), suggesting that the decrease in the density of solitary unmyelinated axons was not simply due to an increase in transverse fascicular area. During this time a large number of solitary axons must become myelinated. The maximum diameter for such solitary axons was reached by 21–23 weeks.

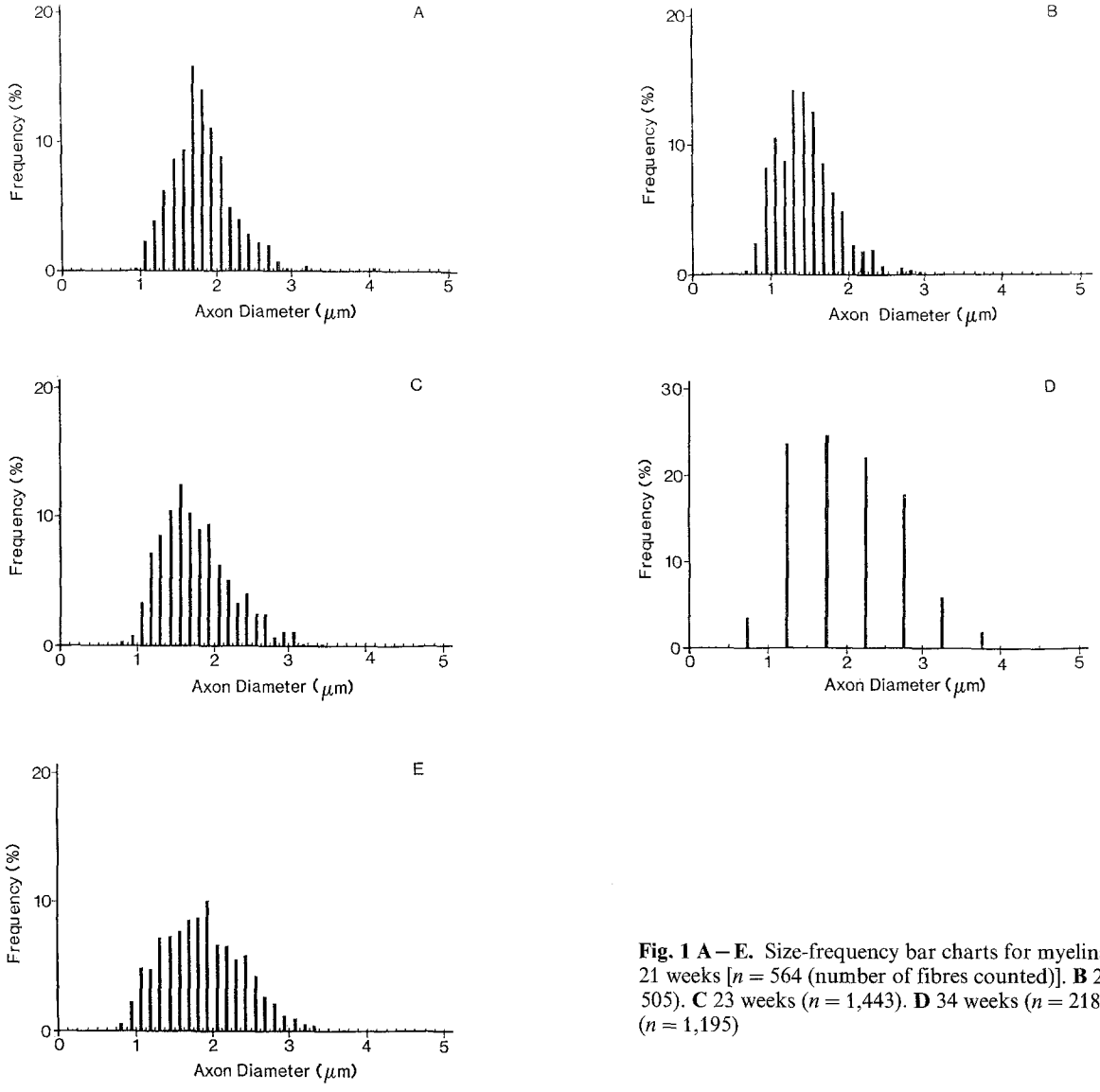

Fig. 1 A–E. Size-frequency bar charts for myelinated fibres. **A** 21 weeks [$n = 564$ (number of fibres counted)]. **B** 22 weeks ($n = 505$). **C** 23 weeks ($n = 1{,}443$). **D** 34 weeks ($n = 218$). **E** 36 weeks ($n = 1{,}195$)

Table 3. Unmyelinated axon morphometry

Age (weeks)	Density of solitary axons (per mm^2) (5–212)[a]	Density of axons in aggregates (per mm^2) (758–2,029)[a]	Density of aggregates[b] (per mm^2) (100–224)[a]	Axons per aggregate			Axon diameters (μm)					
				Mean	Min (100–224)[a]	Max	Solitary			Grouped		
							Mean	Min (5–212)[a]	Max	Mean	Min (740–1,507)[a]	Max
15	3,260	982,591	63,245	14.1	2	44	1.10	0.57	1.33	0.48	0.09	1.99
16	25,382	235,491	31,999	7.0	2	46	—	—	—	—	—	—
21	11,220	555,281	27,367	20.2	2	98	1.65	0.40	2.71	0.49	0.10	1.75
22	18,222	749,310	38,827	16.2	2	54	1.27	0.41	2.46	0.46	0.07	2.60
23	17,650	262,280	27,017	9.7	2	45	1.51	0.67	2.83	0.66	0.12	1.79
33	2,786	197,406	30,871	8.4	2	35	—	—	—	—	—	—
36	4,618	137,370	20,681	6.0	2	25	—	—	—	—	—	— —

[a] Number of axons or aggregates counted
[b] Density of unmyelinated axon aggregates, i.e., Schwann cells enclosing more than one axon

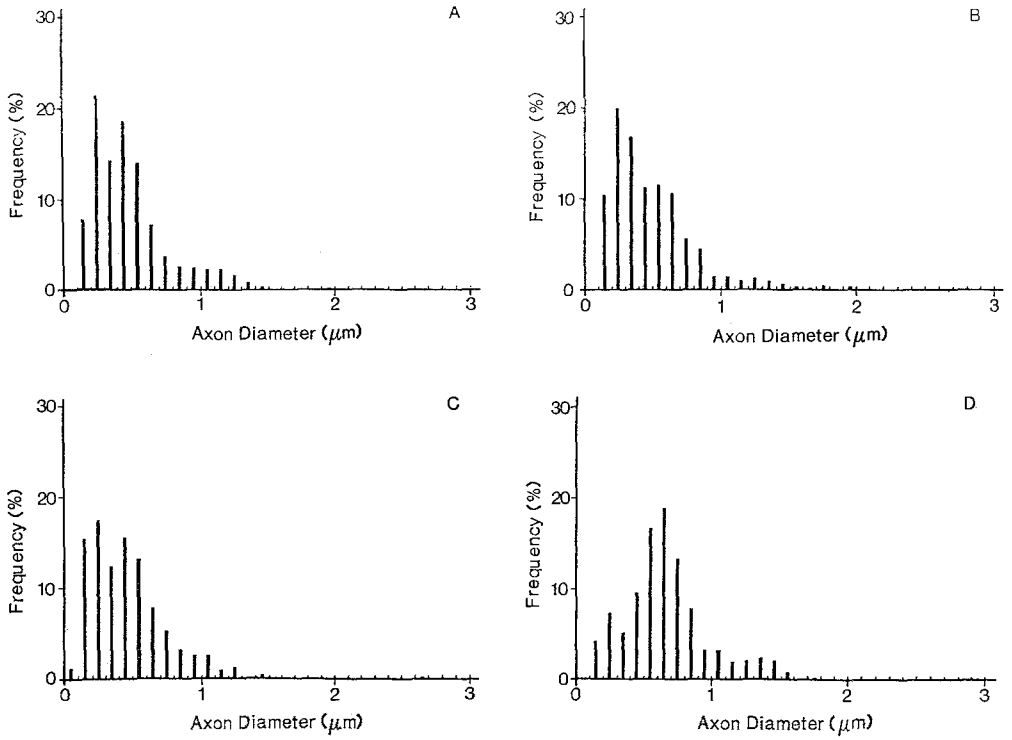

Fig. 2 A–D. Size-frequency bar charts for unmyelinated axons. **A** 15 weeks (n = 1,507). **B** 21 weeks (n = 1,033). **C** 22 weeks (n = 1,250). **D** 23 weeks (n = 740)

Table 4. Schwann cell nuclear density; percentage of fibres cut through nucleus; unmyelinated axon to myelinated fibre and Schwann cell nuclear ratio

Age (weeks)	Schwann cell nuclear density				Percentage of fibres cut through nucleus			UM:M axon ratio			UM:M nuclear ratio		
	Total[a] (per mm^2)	M	UM (S)	UM (A)	M	UM (S)	UM (A)	UM (S)	UM (A)	Total	UM (S)	UM (A)	Total
15	11,736	0	0	11,736	–	–	18.5	–	–	–	–	–	–
16	9,941	0	4,349	5,592	–	17.1	17.4	–	–	–	–	–	–
21	7,699	1,094	2,189	3,831	16.1	19.5	13.9	1.64	81	82	2.00	3.50	5.50
22	8,949	1,186	1,725	6,038	12.5	9.4	15.5	1.92	78	80	1.45	5.09	6.54
23	8,687	1,792	1,930	4,964	11.1	10.9	18.3	1.08	16	17	1.08	2.76	3.84
33	4,759	2,205	116	2,437	7.9	4.1	7.8	0.10	7	7	0.05	1.11	1.16
36	4,362	1,796	171	2,395	7.6	3.7	11.5	0.19	5.8	6	0.10	1.33	1.43

[a] Number of nuclei counted (electron microscopy) = 18–83
M = Myelinated fibres; UM = Unmyelinated fibres; UM (S) = Solitary unmyelinated axons; UM (A) = Aggregates of unmyelinated axons

Unmyelinated axon aggregates. The density of aggregates of unmyelinated axons, packaged together within Schwann cell processes, their diameters, the frequency of aggregates, and numbers of axons per Schwann cell or Schwann cell subunit are given in Table 3. Figure 2 shows the axon diameter-frequency distribution bar charts. Adding the solitary axons to these bar charts did not make a substantial difference to their shape. The density of unmyelinated axon aggregates decreased by a factor of nearly eight from 15 weeks to 36 weeks of age. The fourfold difference in densities at 15 and 16 weeks may be due to intrafascicular variation; Ochoa and Mair (1969a) found a nearly threefold variation due to patchy distribution of unmyelinated axons in their material. The maximum number of axons per Schwann cell was found at 21 weeks, but the number then decreased with increasing age as more axons developed a 1:1 relationship with Schwann cells and became myelinated.

The ratio of solitary and aggregated unmyelinated axons to myelinated axons is shown in Table 4. At 23 weeks there was a drop from 80–82 unmyelinated

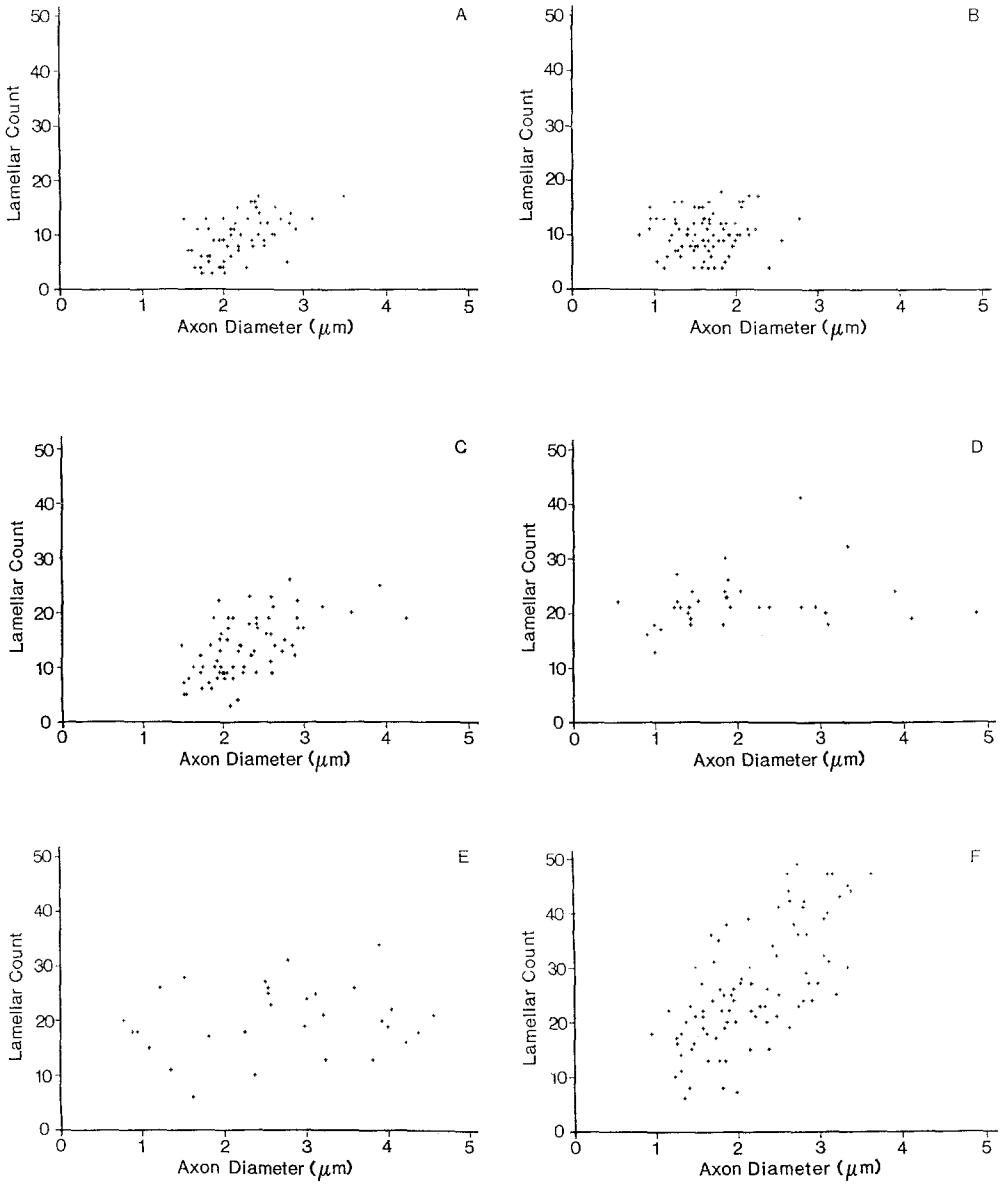

Fig. 3A–F. Relationship between number of myelin lamellae and computed axon diameter. **A** 21 weeks. **B** 22 weeks. **C** 23 weeks. **D** 33 weeks. **E** 34 weeks. **F** 36 weeks

axons per myelinated fibre to 17, followed by a decline to a ratio of 6:1 at 36 weeks.

Nuclei

Table 4 shows the total nuclear density and density related to fibre type. Also shown are the percentages of fibres cut through the nucleus, and the ratio of unmyelinated to myelinated nuclei. The fall in the nuclear density for Schwann cells associated with solitary axons after 23 weeks parallels the fall in axon density (Table 3, column 1). The most prominent change in percentage of Schwann cells cut through the nucleus is for solitary unmyelinated axons.

Discussion

Since the pioneering studies by Geren (1954) on chick embryos, many of the essential features of peripheral nerve morphogenesis (including myelinogenesis) have been elucidated. Nevertheless, there are still only limited morphometric data documenting changes taking place during vital stages of human fetal development.

The time of onset of myelination varies in different human nerves. Dunn (1970) noted the onset of myelination at 14–18 weeks menstrual age in the radial nerve in the axilla, while Cravioto (1965) observed myelination in the sciatic nerve and brachial

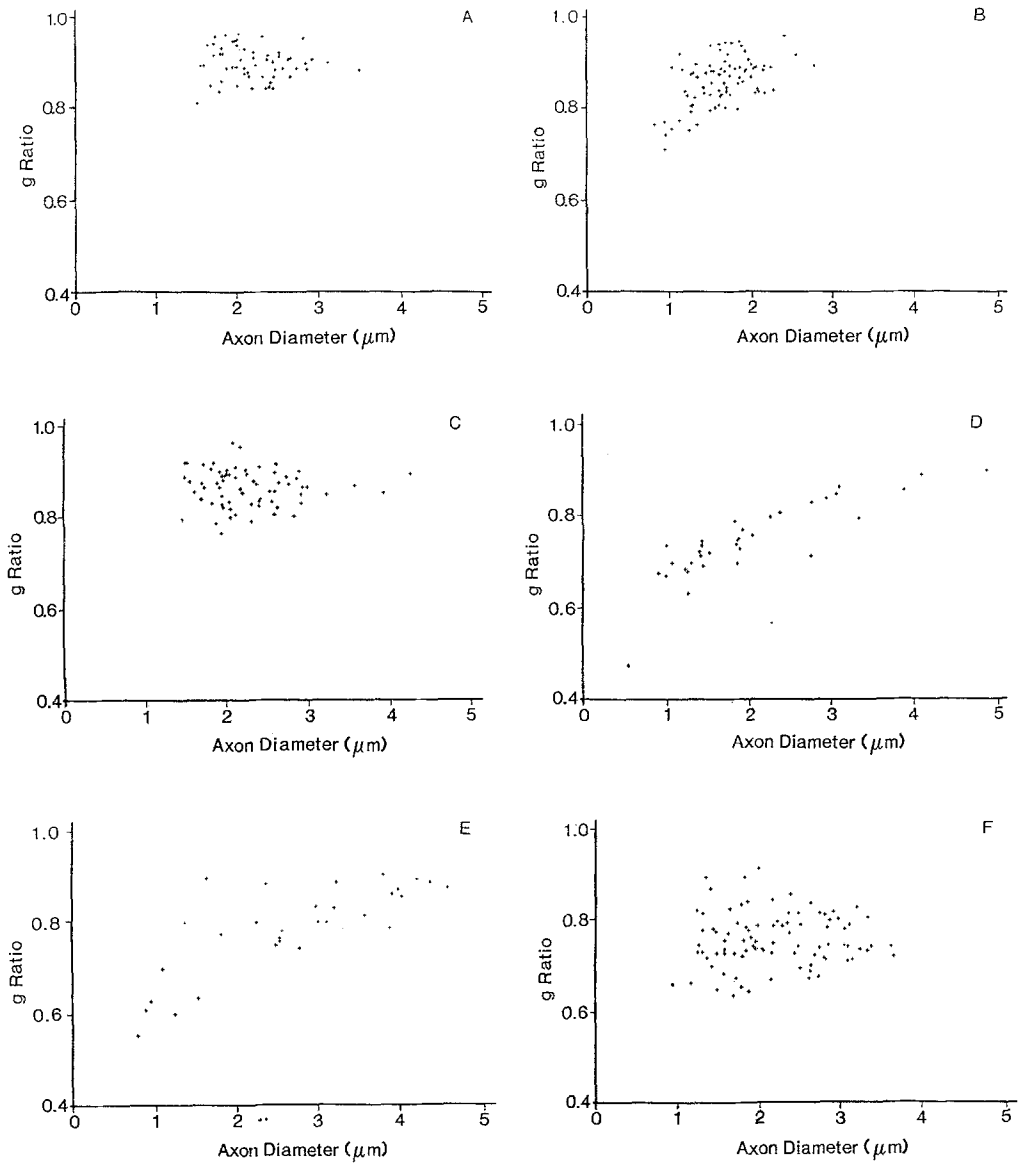

Fig. 4A–F. Relationship between g ratio (axon diameter: total fibre diameter) and computed axon diameter. **A** 21 weeks. **B** 22 weeks. **C** 23 weeks. **D** 33 weeks. **E** 34 weeks. **F** 36 weeks

plexus at 14 to 16 weeks of "intrauterine life". On the other hand, Davison et al. (1973) did not find myelination in sciatic nerve until 18 weeks "ovulation age". In the ulnar nerve just above the elbow, Gamble (1966) found early myelination at 12 weeks menstrual age with well advanced myelination at 16 weeks. Wozniak and O'Rahilly (1981) observed 1:1 Schwann cell:axon development and the onset of myelination in the vagus nerve at 14 weeks postovulation, while by 17 weeks some fibres possessed up to 15 lamellae. In the sural nerve, Ochoa (1971) found that at 18, but not 16, unspecified weeks, axons had established 1:1 relationships with Schwann cells and compact myelin with 15 lamellae was observed. In our material, although at 16 weeks there were many solitary axons surrounded by Schwann cell processes, the formation of compact myelin was not observed. However, by 21 weeks the myelinated fibre density was over 5,000/mm^2 with an average of 9.3 myelin lamellae per sheath. The highest density found by light microscopy was at 36 weeks. Our data combined with those of Gutrecht and Dyck (1970), Tohgi et al. (1977) and Origuchi (1981) suggest that peak myelinated fibre density is reached at or about term, following which it falls to values of approximately 8,000–20,000/mm^2, after infancy but in the first two decades (Tohgi et al. 1977). Adult values have been recorded as 7,000–10,000/mm^2 (Ochoa and Mair 1969a), 7,000 ± 1,600/mm^2

(Behse et al. 1972), $8{,}000 \pm 14{,}000/mm^2$ (Dyck and Gomez 1968), $6{,}130 \pm 1{,}110/mm^2$ (O'Sullivan and Swallow 1968) and $7{,}500 - 10{,}000/mm^2$ (Jacobs and Love 1985). Values vary with, among other factors, the method of fixation (Gutrecht and Dyck 1970; Tohgi et al. 1977) and section thickness. The fall in myelinated fibre density post-term is presumably mainly due to an increase in transverse fascicular area which, in Origuchi's (1981) study, increased from 0.138 mm^2 at 4 days to 0.556 mm^2 at 3 years. Gutrecht and Dyck (1970) found an increase in area from 0.16 mm^2 at 5 weeks premature to 0.77 mm^2 at 14 years, and Jacobs and Love (1985) an increase from $0.2 - 0.3$ mm^2 in neonates to $0.6 - 1.2$ mm^2 in adults. A range of $0.55 - 1.55$ mm^2 in adults was obtained by Behse et al. (1972).

While the density of myelinated fibres in the present series increased substantially from 21 to 36 weeks, the mean and maximum axon diameters of these fibres did not increase, the mean diameter remaining in the $1.5 - 2.0$ μm range. At the same time, however, the mean lamellar count almost trebled. Schröder et al. (1978) found that mean axon diameter varied only within the range of $2.15 - 2.65$ μm in the last 2 months of pregnancy, although the value in their single fetus 4 months preterm was 1.63 μm.

The myelinated axon diameter frequency distribution curves for all nerves were unimodal, a finding consistent with other studies. Origuchi (1981) found unimodal histograms at 18 months and 23 months but bimodality at 3 years and concluded that the age at which bimodality appears is probably about 2 years. Tohgi et al. (1977), however, found that large myelinated fibres first appeared at 5 months of age and that the density of these fibres increased up to adult levels at approximately 3 years. The 7-month-old nerve studied by Gutrecht and Dyck (1970) showed a distinct peak at $5.0 - 5.9$ μm, this peak shifting to $8.0 - 8.9$ μm by 10 years of age. These authors concluded that axons of the large fibre group attain adult diameters just after 5 years of age, a conclusion also reached by Schröder et al. (1978). Definite bimodality was observed after about 1 year by Jacobs and Love (1985).

Ochoa (1971) found that the most striking change between nerves at 16 and 18 weeks was that some axons became the sole occupants of the Schwann cell, a process heralding the onset of myelination. He found up to 15 myelin lamellae at 18 weeks, but in our material maximum lamellar counts of 17 and 18 were only reached by 21 and 22 weeks respectively. Thereafter the lamellar count progressively increased. From our data and those of Schröder et al. (1978) it appears that the mean lamellar count increases two- to threefold during the last 4 months of gestation, twofold during the first 2 years of postnatal life and one and a halffold over the ensuing 12 years. The early rapid increase in lamellar counts occurs preterm when the mean axon diameter is changing very little, whereas over the next 2 years the lamellar count increase slows as the larger diameter fibre population establishes itself. The explanation for this differential growth pattern between axons and myelin is uncertain. Changes in myelin sheath thickness in relation to axon diameter can only be adequately understood if related to myelin segment length (Friede and Bischhausen 1982). In the present investigation, measurement of internodal length in teased fibre preparations was not feasible because of the small calibre of the fibres.

Counting the number of lamellae in a myelin sheath is an advantageous way of minimizing errors inherent in the direct measurement of myelin sheath thickness (Friede and Samorajski 1967; Dyck et al. 1971), while the g ratio has been used to express the relationship of axon diameter to total fibre diameter. The relationship between myelin thickness (or lamellar count), or the g ratio, and axon diameter, has been studied in animals and humans. The varying results have been summarized by Thomas and Ochoa (1984). Gutrecht and Dyck (1970) found in normal human sural nerves in the first two decades that there was a linear relationship between axon diameter and total fibre diameter, and that there was no change in this relationship with increasing age (5 weeks premature to 10 years). The g ratio for large fibres was higher than that for small fibres, but these authors felt that the result might be produced by varying thickness of sections and obliquity of fibres affecting the ratio in small fibres (Dyck et al. 1968). Subsequently, Dyck et al. (1971) found in sural nerves ($7 - 66$ years) that large axons have relatively more myelin lamellae than smaller axons and that myelin was thinner in two nerves at 7 and 10 years than in the older nerves.

Noting the lack of uniformity of previous findings, Schröder et al. (1978) performed a study of axon calibre and myelin sheath thickness in the sural nerve from 5 months gestation to 15 years. They found asynchronous development, with axon diameter increasing to a peak at 5 years of age and myelin thickness increasing more slowly up to 14 years. Axons of equal size had more myelin in older than in younger children.

In our material, a significant linear relationship was found between lamellar counts and axon diameters only at 21, 23 and 36 weeks. Schröder et al. (1978) noted that in their younger age group the smaller diameter axons showed a strikingly wide scatter of axonal diameters with equal numbers of lamellae and that the regression line for the lamellar count compared with axon circumference was less

steep if only the small fibre groups were used. Hence it may not be surprising that a significant correlation was not found in all of our nerves. Other potential factors for the lack of a uniform finding include distortion due to the variation in time before fixation, the small range (essentially 1–2 μm) of axon sizes in the nerve at 22 weeks and the small number of fibres studied at 33 and 34 weeks.

Scattergrams showed no correlation of the g ratio with axon diameter at 21, 23 and 36 weeks, but a linear correlation did exist in the nerves at 22, 33 and 34 weeks. This finding could be anticipated from the lamellar count data in that, if the lamellar count (i.e., sheath thickness) did not increase with increasing axon diameter, then the sheath thickness remains relatively thin and the g ratio increases. In an infant at one month, Friede and Beuche (1985) found a mean g ratio of 0.80 with the scattergram showing a homogeneous cluster of values without a clear-cut regression for sheath thickness with fibre calibre. By 2–4 years of age they found separation in the scattergram which defined a population of large fibres with lower g ratios (thicker myelin) and one of smaller fibres with higher g ratios (thinner myelin). Similar findings were obtained by Jacobs and Love (1985).

The few electron microscope studies available of sural nerve unmyelinated fibre densities have shown a drop from 235,000/mm^2 at birth to 60,000–80,000/mm^2 at 3–10 years (Origuchi 1981), followed by a decline to 22,000–34,000/mm^2 in persons of 15–22 years (Ochoa and Mair 1969a). Jacobs and Love (1985) found that the density fell from 150,000–200,000/mm^2 at birth to about 50,000/mm^2 at 2 years and then to 30,000–40,000/mm^2 at 10 years. Ochoa and Mair (1969a) noted variation between different areas in the nerve could be almost threefold. It is possible that the density differences between our nerves at 15 and 16 weeks could be explained on this basis. The densities from 15–23 weeks were higher than those from 33 weeks onwards, but when the package density (i.e., the density of Schwann cells or subunits containing more than one axon) is considered rather than axon density, the decline is less considerable.

The young adult pattern of predominantly one or two unmyelinated axons per Schwann cell subunit (Ochoa and Mair 1969a) evolves by division of Schwann cells with progressive sequestration of the large aggregates of axons so characteristic of early fetal life, into smaller and smaller packages. In Ochoa's (1971) 9-week specimen, aggregates contained approximately 800 axons, decreasing to 50–150 at 16 weeks. The number declined to a mean of six axons per Schwann cell or Schwann cell subunit at 36 weeks in our material. Hence, even at this stage, further time is required for the segregation process and the age at which the adult pattern is achieved is not known.

The first quantitative electron microscopy analysis of unmyelinated fibres in an infant appears to be that of Weller (1967), who measured 200 axons in a 6-month-old infant and found the peak to be at 1.5–2.0 μm with a range of 0.5–3.0 μm. Subsequently, Origuchi (1981) found the unmyelinated fibre diameter histogram from birth to 10 years to be unimodal with the peak usually at 0.3–0.5 μm. In an 18-week fetus Ochoa (1971) found axon diameters ranging from 0.1–3.2 μm with the main peak at 0.4 μm. The smallest unmyelinated axons occurring alone in a Schwann cell were 0.6 μm in diameter while the largest devoid of myelin were 3.2 μm. In our material, solitary unmyelinated axons ranged in diameter from just under 0.1 μm to 2.83 μm, axons of aggregates having a maximum diameter of 2.6 μm. The smallest sole unmyelinated occupant of a Schwann cell or subunit was 0.4 μm in diameter. Unfortunately preservation of unmyelinated axons in the older fetuses was not good enough to justify diameter measurements (although satisfactory for counting numbers). However, the data suggest that unmyelinated axons reached their maximum diameters by at least 23 weeks gestation. Ochoa (1971) reached the same conclusion, observing that the maximum diameter of unmyelinated axons in his 18 week fetus was similar to that in adults, i.e., 3.0 μm, but rarely more than 2.8 μm (Ochoa and Mair 1969a).

The ratio of total unmyelinated axons to myelinated fibres dropped from 82:1 at 21 weeks to 6:1 at 36 weeks, well above the value of 3.7:1 for young adults (Ochoa and Mair 1969a). This suggests that at birth and in early infancy not only are myelinated fibres increasing their sheath thickness, but that previously unmyelinated axons are still initiating the myelination process. Origuchi (1981) concluded that the ratio might be close to adult values at about 2 years.

The probability of a section passing through a Schwann cell nucleus depends on the thickness of the section, Schwann cell spacing and the length of the nucleus itself. As there is a direct relationship between internodal length in myelinated fibres and fibre diameter (Thomas and Ochoa 1984), it is not surprising that nuclear density should be relatively high in fetal nerve with its high density of small fibres (Gamble and Breathnach 1965). Ochoa and Mair (1969a) found in young adults that Schwann cell nuclear density on electron microscopy was 2,431/mm^2, with 76.1% belonging to unmyelinated fibres and 19.1% to myelinated fibres. About 90% of all nuclei belonged to Schwann cells. Tohgi et al. (1977), in a light

microscope study, gave a Schwann cell nuclear density of 9,800/mm^2 at 1 week of age (postnatal) falling to 3,570/mm^2 in the second decade. These values are higher than our electron microscope-based calculation of 11,736/mm^2 at 15 weeks and 4,363/mm^2 at 36 week postovulation. The density of Schwann cell nuclei associated with myelinated fibres changed relatively less with increasing age compared with the increasing myelinated fibre density, this presumably representing mainly a balance between increasing density and increasing internode length due to growth of the limb, and is reflected in the decreasing percentage of myelinated fibres cut through the nucleus. The values of 7.6–9.3% for the three older nerves are similar to those found by Ochoa and Mair (1969a) by light microscopy for small myelinated fibres in young adults. The most striking change in percentage of fibres cut through the nucleus was for fibres associated with solitary unmyelinated axons with a change from 19.5% at 21 weeks to 3.7% at 36 weeks. At the same time there was no increase in the mean or maximum diameters of these fibres to account for the observed change.

Acknowledgements. We acknowledge the assistance of Mr. John Muddle and helpful discussion with Dr. J. Ochoa and Professor J. M. Schröder. The electron microscope was provided by the Medical Research Council and technical help by Jackie O'Neill and Jane Workman. The investigation was approved by the Ethics Committee of the Royal Free Hospital. We thank Professor R. Shaw and Dr. G. Burford, Department of Obstetrics and Gynaecology, Royal Free Hospital School of Medicine and Dr. J. Keeling, Department of Pathology, The John Radcliffe Hospital, Oxford, for provision of fetal material.

References

Behse F, Buchthal F, Carlsen F, Knappeis GG (1972) Hereditary neuropathy with liability to pressure palsies. Brain 95:777–794

Behse F, Buchthal F, Carlsen FM, Knappeis GG (1975) Unmyelinated fibres and Schwann cells of sural nerve in neuropathy. Brain 98:493–510

Cravioto H (1965) The role of Schwann cells in the development of human peripheral nerves. An electron microscope study. J Ultrastruct Res 12:634–651

Davison AN, Duckett S, Oxbury JM (1973) Correlative morphological and biochemical studies of the human fetal sciatic nerve. Brain Res 58:327–342

Dunn JS (1970) Developing myelin in human peripheral nerve. Scott Med J 15:108–117

Dyck PJ (1966) Histological measurements and fine structure of biopsied sural nerve: normal, and in peroneal muscular atrophy, hypertrophic neuropathy and congenital sensory neuropathy. Mayo Clin Proc 41:742–774

Dyck PJ, Gomez MR (1968) Segmental demyelination in Dejerine-Sottas disease: light, phase-contrast, and electron microscopic studies. Mayo Clin Proc 43:280–296

Dyck PJ, Gutrecht JA, Bastron JA, Karnes WE, Dale AJD (1968) Histologic and teased-fiber measurements of sural nerve in disorders of lower motor and primary sensory neurons. Mayo Clin Proc 43:81–123

Dyck PJ, Lambert EH, Sanders K, O'Brien PC (1971) Severe hypomyelination and marked abnormality of conduction in Dejerine-Sottas hypertrophic neuropathy: myelin thickness and compound action potential of sural nerve in vitro. Mayo Clin Proc 46:432–436

Eames RA, Gamble HJ (1970) Schwann cell relationships in normal human cutaneous nerve. J Anat 106:417–435

Friede RL, Beuche W (1985) Combined scatter diagrams of sheath thickness and fibre calibre in human sural nerves: changes with age and neuropathy. J Neurol Neurosurg Psychiatry 48:749–756

Friede RL, Bischhausen S (1982) How are sheath dimensions affected by axon caliber and internode length? Brain Res 235:335–350

Friede AL, Samorajski T (1967) Relation between the number of myelin lamellae and axon circumference in fibers of vagus and sciatic nerves. J Comp Neurol 130:223–232

Friede AL, Samorajski T (1968) Myelin formation in the sciatic nerve of the rat. A quantitative electron microscopic histochemical and radioautographic study. J Neuropathol Exp Neurol 27:546–570

Gamble HJ (1966) Further electron microscope studies of human foetal peripheral nerves. J Anat 100:487–502

Gamble HJ, Breathnach AS (1965) An electron-microscope study of human foetal peripheral nerves. J Anat 99:573–584

Geren BB (1954) The formation from the Schwann cell surface of myelin in the peripheral nerves of chick embryos. Exp Cell Res 7:558–562

Gutrecht JA, Dyck PJ (1970) Quantitative teased-fiber and histologic studies of human sural nerve during postnatal development. J Comp Neurol 138:117–130

Jacobs JM, Love S (1985) Qualitative and quantitative morphology of human sural nerve at different ages. Brain (in press)

Ochoa J (1971) The sural nerve of the human foetus: electron microscopic observations and counts of axons. J Anat 108:231–245

Ochoa J, Mair WGP (1969a) The normal sural nerve in man. I. Ultrastructure and numbers of fibres and cells. Acta Neuropathol (Berl) 13:197–216

Ochoa J, Mair WGP (1969b) The normal sural nerve in man. II. Changes in the axons and Schwann cells during ageing. Acta Neuropathol (Berl) 13:217–239

Origuchi Y (1981) Quantitative histological study in the sural nerves of children. Brain Dev 3:395–402

O'Sullivan DJ, Swallow M (1968) The fibre size and content of the radial and sural nerves. J Neurol Neurosurg Psychiatry 31:464–470

Schmitt FO, Bear RS (1937) Optical properties of the axon sheaths of crustacean nerves. J Cell Comp Physiol 9:261–275

Schröder JM, Bohl J, Brodda K (1978) Changes of the ratio between myelin thickness and axon diameter in the human developing sural nerve. Acta Neuropathol (Berl) 43:169–178

Sharma AK, Thomas PK (1975) Quantitative studies on age changes in unmyelinated fibres in the vagus nerve of man. In: Kunze K, Desmedt JE (eds) Studies on neuromuscular diseases. Karger, Basel, pp 211–219

Sievers J (1971) Basic two-dye stains for epoxy-embedded 0.3–1 μ sections. Stain Technol 46:195–199

Streeter GL (1920) Weight, sitting height, head size, foot length, and menstrual age of the human embryo. Contrib Embryol (Carnegie Inst Wash) 11:143–170

Thomas PK, Ochoa J (1984) Microscopic anatomy of peripheral nerve fibers. In: Dyck PJ, Thomas PK, Lambert EH, Bunge

R (eds) Peripheral neuropathy, 2nd edn. Saunders, Philadelphia, pp 39–96

Tohgi HH, Tsukagoshi H, Toyokura Y (1977) Quantitative changes with age in normal sural nerves. Acta Neuropathol (Berl) 38:213–220

Weller RO (1967) An electron microscopic study of hypertrophic neuropathy of Dejerine and Sottas. J Neurol Neurosurg Psychiatry 30:111–125

Wozniak W, O'Rahilly R (1981) Fine structure and myelination of the developing human vagus nerve. Acta Anat (Basel) 109:218–230

Wozniak W, O'Rahilly R, Bruska M (1982) Myelination of the human fetal phrenic nerve. Acta Anat (Basel) 112:281–296

Received December 4, 1985/Accepted December 31, 1985